

Corrosion Inhibition of Copper and Copper Alloy in 3M Nitric Acid Solution using Organic Inhibitors

O.R.M. Khalifa, A.K. Kassab, H.A. Mohamed and S.Y. Ahmed

Chemistry department, Faculty of Girls for Arts, Science and Education, Ain shams University, Cairo, Egypt

Abstract: The effect of the addition of organic compounds containing an amino group, such as ethylamine (EA), ethylenediamine (EDA) and butanediamine (BDA), on the corrosion of copper and copper alloy in nitric acid was studied by weight loss, open circuit potential and potentiodynamic polarization techniques. The explored methods gave almost similar results. Results obtained revealed that butanediamine is the best inhibitor and the protection efficiency (p%) follows the sequence butanediamine > ethylenediamine > ethylamine. The effect of temperature on the corrosion behavior of copper and copper alloy in nitric acid solution in presence and absence of inhibitor were studied in the temperature range 30-60°C. The associated activation corrosion and free adsorption energies have been determined. SEM examination of the copper and copper alloy surface revealed that these compounds prevented copper and copper alloy from corrosion by adsorption on its surfaces. [Journal of American Science 2010;6(8):487-498]. (ISSN: 1545-1003).

Keywords: Copper; Copper alloy; Nitric acid; Corrosion inhibition; Amines

1. Introduction

Copper and its alloys have many industrial applications such as electronics because of their excellent corrosion resistance properties as well as their superior electrical and thermal performance [1]. Although copper is malleable and machinable, it is not very durable. If a high strength material is desired, copper has to be alloyed with other metals, such as zinc, tin, aluminum or nickel [1]. Doping with divalent cations is an effective way of improving the corrosion resistance of copper. Chemical dissolution and electrolytic plating are the main processes used in the fabrication of electronic devices. The most widely used corrosive solution contains nitric acid, so this medium has induced a great deal of research on copper corrosion [2-6]. One of the most important methods in the corrosion protection of copper is the use of organic inhibitors [7-9]. Most of the excellent acid inhibitors are organic compounds containing nitrogen, sulfur and oxygen [10-18], and heterocyclic compounds with polar functional groups and conjugated double bonds [19-23]. The inhibiting action of these organic compounds is usually attributed to their interactions with the copper surface via their adsorption. Polar functional groups are regarded as the reaction center that stabilizes the adsorption process [24]. In general, the adsorption of an inhibitor on a metal surface depends on the nature and the surface charge of the metal, the adsorption mode, its chemical structure, and the type of the electrolyte solution [25]. Amines are known to be very effective inhibitors for metals and alloys in different corrosion media. Srivastava et al [26] found that 0-, m- and p-phenylenediamine show effective inhibition efficiencies. The aim of the

present investigation was to study the inhibitive action of some aliphatic amines on the corrosion of copper in the aerated 3M nitric acid solution.

2. Experimental

The investigation of inhibiting properties of butanediamine (BDA), ethylenediamine (EDA) and ethylamine (EA) (Aldrich) were performed using the weight loss method and electrochemical studies, including open-circuit potential and potentiodynamic polarization techniques, along with scanning electron microscopy (SEM). Both copper (99.9% Cu) and copper alloy (65% Cu- 10% Ni- 25% Zn) were tested in 3 M nitric acid solution. The latter is of analytical grade and has been used without further purification. Double distilled water was used in the preparation of solutions. Prior to all measurements, the substrates were etched in a 6 M nitric acid solution for 20 sec, then washed thoroughly with distilled water, degreased with ethanol, washed again with distilled water and finally dried at room temperature. The specimens were weighted and immersed in the corrosive medium.

The weight loss measurements were carried out at 30, 40, 50 and 60°C using sheets of the substrates with dimensions 2 x 2.5 cm². The sheets were suspended in 20 mL solution of 3 M nitric acid with and without the different inhibitors concentrations (0.001-1 M) for 30 minute. The loss in weight per area A (=10 cm²) in mg/cm² (W_i), the corrosion rate (R_{corr}), and the percentage of protection efficiency (P%) were calculated over different inhibitors concentrations according to the following equations:

$$W_t = \frac{W_o - W_1}{A} \quad (1)$$

$$R_{\text{corr}} = \frac{W_t}{t} \quad (2)$$

$$P\% = \left[1 - \left(\frac{R'_{\text{corr}}}{R_{\text{corr}}} \right) \right] \times 100 \quad (3)$$

where W_o is the original weight (mg) and W_1 the weight after immersion in the test electrolyte, t the immersion time (sec), and R'_{corr} and R_{corr} are corrosion rates with and without an inhibitor, respectively.

Two measurements were performed in each case and the mean value of the weight loss was reported. The open circuit potential (OCP) was measured using pH-meter-millivoltmeter type WGPYE model 290. The OCP of copper and the copper alloy were measured versus (SCE) saturated calomel electrode as a function of immersion period in 3 M nitric acid in the presence and absence of amine derivatives till steady state values were reached.

Potentiodynamic polarization studies were carried out with the test specimens having an exposed area of 1 cm² using EG&G PARC model 350A (console) in the range from -250 mv to 1000 mv using a scan rate of 0.5 mV/sec. The cell consisted of test specimens as working electrode and (SCE) as reference electrode. Two carbon electrodes were used as counter electrodes.

Scanning electron microscope (SEM) unit "JEOL JSM5410" was used to demonstrate the surface morphology of different samples employing an accelerating voltage of 30 kv. Samples were mounted using carbon paste to ground them. The results were obtained as computer print out.

3. Results and Discussion:

3.1- Weight loss measurement

Fig.1 and Fig. 2 show the average corrosion rate (R_{corr}) of copper and copper alloy sheets, expressed as mg sec⁻¹ cm⁻², as a function of the logarithmic concentration of BDA, EDA and EA in 3 M HNO₃ solution at 30°C, respectively. They demonstrate that the addition of the organic inhibitors decreases the corrosiveness of the acid. The corrosion rate of copper and copper alloy depends on the concentration of inhibitors. Their action depends on the nature of substituent. Fig. 3 and Fig. 4 show the variation of the protection efficiency of copper and copper alloy respectively as a function of the logarithmic concentration of BDA, EDA and EA in 3 M HNO₃ solution at 30°C. The protection efficiency increases with increasing inhibitors concentrations.

Also, the protection efficiency increases from EA to EDA to BDA as shown in Table (1).

Fig. 5 and Fig. 6 show the variation of corrosion rate of copper and copper alloy, respectively, as a function of the logarithmic concentrations of BDA at different temperatures. Fig. 7 and Fig. 8 show the effect of the concentration of BDA on the protection efficiency of copper and copper alloy, respectively, at various temperatures. The same behaviour is observed for EDA and EA. In general, the protection efficiency increases with decreasing temperature. This indicates that the adsorption of these compounds on copper and copper alloy surfaces is a physical adsorption.

3.2- Adsorption isotherm

In order to obtain a better understanding of the electrochemical process on the metal surface, adsorption isotherms at 30°C were drawn. The degree of surface coverage (θ) at different concentration of each inhibitor in acidic medium has been evaluated from weight loss measurement according to equation (4).

$$\theta = \left[1 - \left(\frac{R'_{\text{corr}}}{R_{\text{corr}}} \right) \right] \quad \dots\dots\dots (4)$$

Data related to the degree of the surface coverage (θ) were tested graphically in order to determine the most suitable adsorption isotherm.

As shown in Fig.9 and Fig.10 the plot of C / θ versus C for copper and copper alloy in 3M HNO₃ with different inhibitors concentrations, yields a straight line showing that the adsorption of these inhibitors is well described by the Langmuir isotherm. These isotherms are described by equation 5.

$$\frac{C}{\theta} = \frac{1}{k} + C \quad \dots\dots\dots (5)$$

$$k = \frac{1}{55.5} \exp \left(\frac{-\Delta G^\circ}{RT} \right) \quad \dots\dots\dots (6)$$

where C is the inhibitor concentration, k the adsorption constant, and G° the standard free energy of adsorption.

The calculated values of k and G° of the adsorption reaction for copper and copper alloy are shown in Table (2). The negative value of the standard free energy of adsorption indicates spontaneous adsorption of these inhibitors on copper and copper alloy. This means that the inhibitive action of these substances results from the physical adsorption [27] as mentioned before.

3.3- Activation Energy

According to the Arrhenius equation, the apparent activation energy, E_a ; for the corrosion process can be determined from the slope of logarithm corrosion rate, $\log R_{corr}$, against $1/T$.

$$\ln R_{corr} = \ln A + \frac{-E_a}{RT} \quad (7)$$

where A is the pre-exponential parameter of Arrhenius. Fig. 11 and Fig.12 show the logarithmic plot of the corrosion rate of copper and copper alloy in 3M HNO_3 as a function of $(1/T)$ in free and inhibited solutions respectively. For the inhibitor free solution, the energy of activation, evaluated from these graphs, is found to be equal to 5.733 and 7.644 KJ mol⁻¹ for copper and copper alloy, respectively. These values are in agreement with the literature data [28]. In the presence of anyone of the studied inhibitors, the energy of activation increases. For a 0.3M concentration of BDA, EDA and EA, the calculated values of the apparent activation energies are 15.28, 12.74 and 9.55 KJ/mol for copper respectively, and 22.93, 19.11 and 15.28 for copper alloy, respectively. This indicates that the formation of the adsorption film occurs by a physical mechanism [29].

By plotting $\log (R_{corr}/T)$ vs. $(1/T)$ at 0.3M of the tested inhibitors, straight lines are obtained for copper and copper alloy as shown in Fig.13 and Fig.14 respectively. The values of H° and S° can be calculated from the slopes and intercepts of the straight lines, respectively, Table (3).

These results indicate that copper metal suffers from more corrosion than copper alloy. This observation may be attributed to the relatively high resistance of copper alloy due to the presence of nickel. S in the presence of additives is larger, meaning that a decrease in disorder takes place in going from reactant to the activated complex [30, 31].

3.4. Open circuit potential (OCP) measurements:

Copper and copper alloy sheets were kept for 2 hour in 3 M HNO_3 solution in the absence and presences of the tested inhibitors. The variation of the steady state potential (E_h) with the logarithm concentration of the tested inhibitors for copper and copper alloy is represented by Fig. 15 and Fig. 16. It is clear from these curves that, as the inhibitor concentration increases, there is a shift in the steady state potential to less positive or more negative direction (relative to the blank).

3.5. Potentiodynamic polarization measurements:

Fig. 17 and Fig. 18 show the potentiodynamic polarization curves of copper and copper alloy in 3M HNO_3 in the absence and in the presence of the different inhibitors under investigation. The figures show that the cathodic current potential curves give rise to parallel Tafel lines indicating that the hydrogen evolution reaction is activation controlled and the addition of the studied inhibitors does not modify the mechanism of this process (The adsorbed molecules of studied inhibitors have no effect on the mechanism of either copper or copper alloy dissolution or hydrogen evolution reaction).

The value of corrosion potential (E_{corr}) is modified by the addition of compounds studied. The addition of compounds studied decreases the current densities in a large domain of anodic and cathodic potentials.

3.6. Scanning electron microscope:

Fig. 19 and Fig. 20 show the morphological images of copper and copper alloy after 1 hour in 3M HNO_3 solution free and with 1 % of EA, EDA or BDA. It is clear that the corrosion attack was more pronounced in absence of additives, while by the addition of different inhibitors the film formed on copper and copper alloy surfaces becomes more protective. The protective film is more pronounced for BDA > EDA > EA.

Table 1: The protection efficiency of different inhibitors in 3M HNO_3 solution calculated from equation 1, at 30°C

Inhibitors	Protection efficiency	
	Copper	Coppr alloy
Butandiamine	99.66	99.90
Ethylenediamine	99.19	99.27
Ethyl amine	87.18	88.10

Table 2: The calculated K and G° of the adsorption reaction for copper and copper alloy in presence of different inhibitors in 3M HNO_3 solution, at 30°C

Inhibitors	Copper		Copper alloy	
	K (L mol^{-1})	G° (kJ mol^{-1})	K (L mol^{-1})	G° (kJ mol^{-1})
Butandiamine	2750.00	-30.02	2000.00	-29.22
Ethylenediamine	1100.10	-27.71	1000.00	-27.47
Ethyl amine	613.40	-26.24	546.40	-25.95

Table 3: Thermodynamic parameters for the adsorption of different inhibitors on copper and copper alloy surfaces in 3M HNO_3 solution.

Inhibitors	Copper		Copper alloy	
	H_{ads} , KJ mol^{-1}	$-S_{\text{ads}}$, $\text{J mol}^{-1}\text{K}^{-1}$	H_{ads} , KJ mol^{-1}	$-S_{\text{ads}}$, $\text{J mol}^{-1}\text{K}^{-1}$
Butandiamine	15.288	8.881	24.843	10.292
Ethylenediamine	11.466	8.051	19.110	8.47
Ethyl amine	9.555	7.138	15.288	7.47

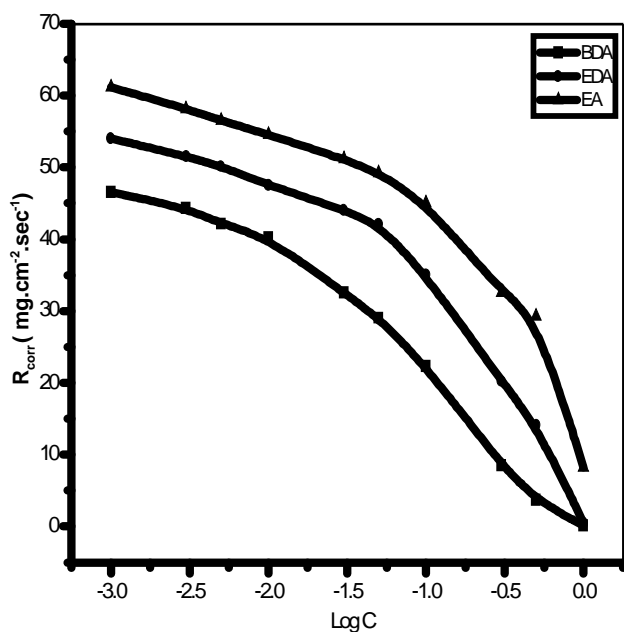


Fig.(1): The corrosion rate of copper in 3M HNO_3 solution in presence of different concentration of BDA, EDA and EA.

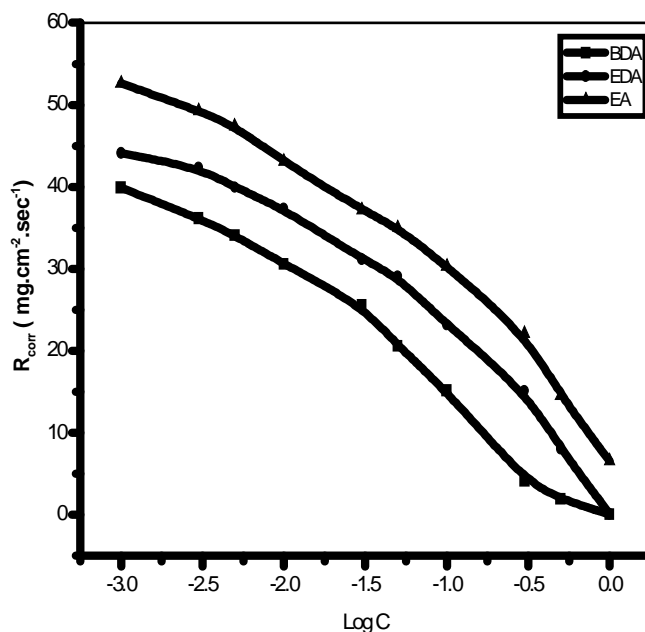


Fig.(2): The corrosion rate of copper alloy in 3M HNO_3 solution in presence of different concentration of BDA, EDA and EA.

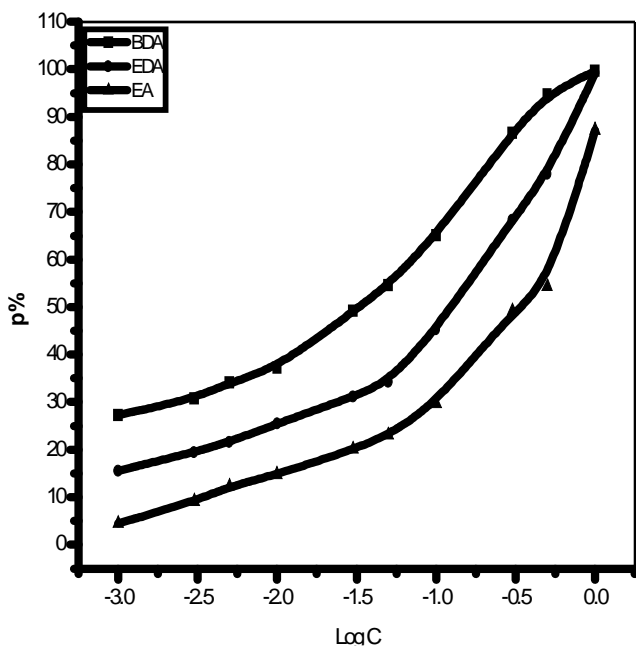


Fig.(3): The protection efficiency of copper in 3M HNO₃ solution in presence of different concentration of BDA,EDA and EA.

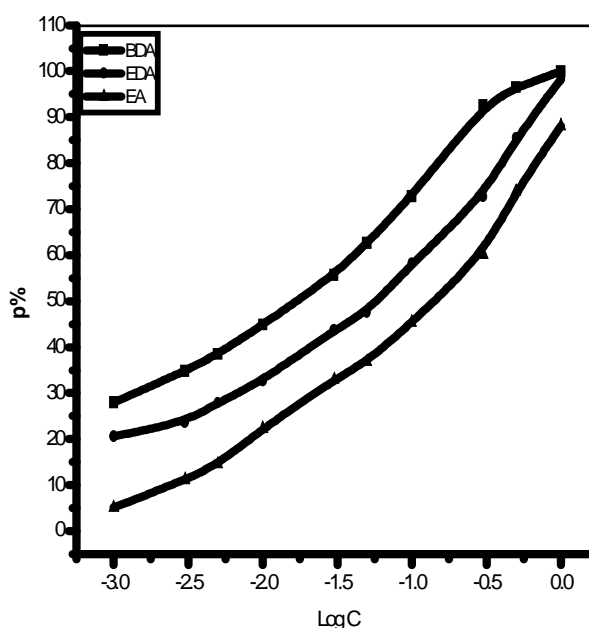


Fig.(4): The protection efficiency of copper alloy in 3M HNO₃ solution in presence of different concentration of BDA,EDA and EA.

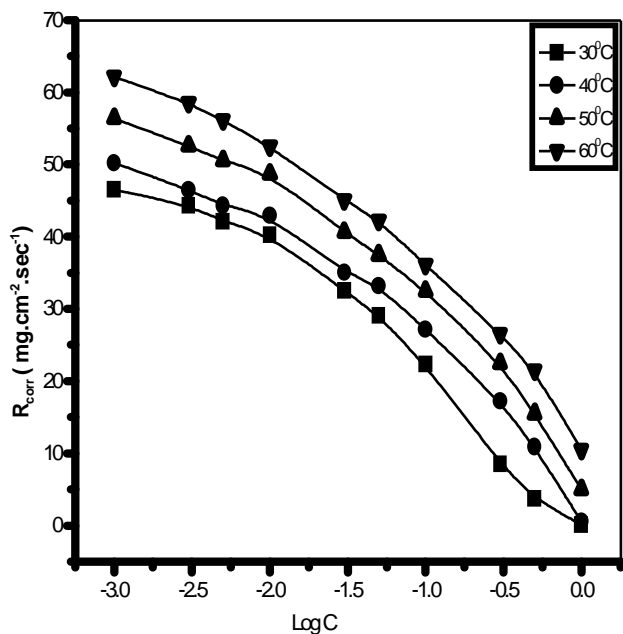


Fig.(5): The corrosion rate of copper in 3M HNO₃ solution in presence of different concentration of BDA, at different temperature

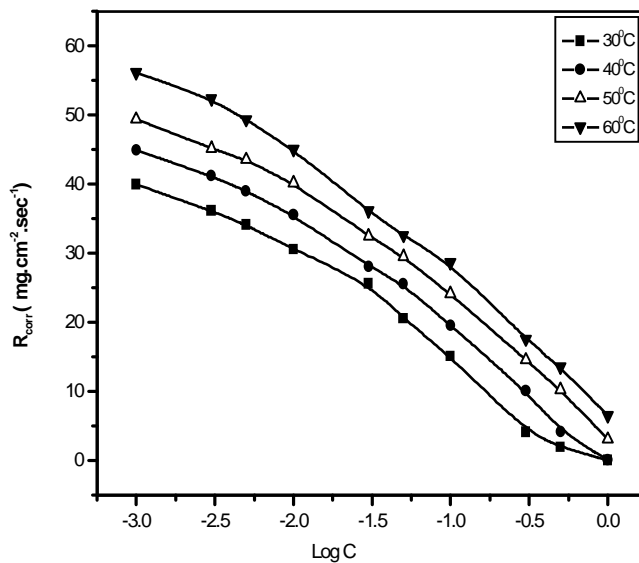


Fig.(6): The corrosion rate of copper alloy in 3M HNO₃ solution in presence of different concentration of BDA at different temperature.

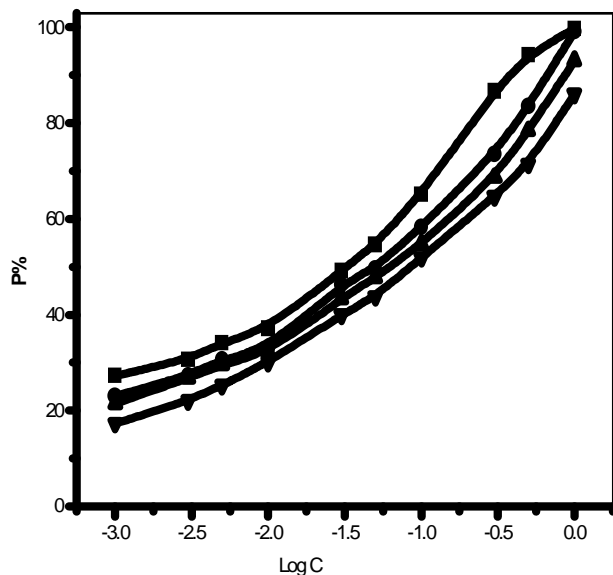


Fig.(7): The protection efficiency of copper in 3M HNO₃ solution in presence of different concentration of BDA at different temperature.

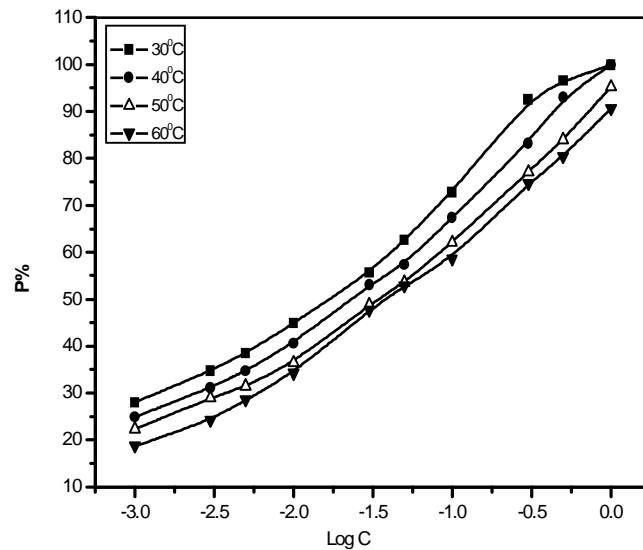


Fig.(8): The protection efficiency of copper alloy in 3M HNO₃ solution in presence of different concentration of BDA at different temperature.

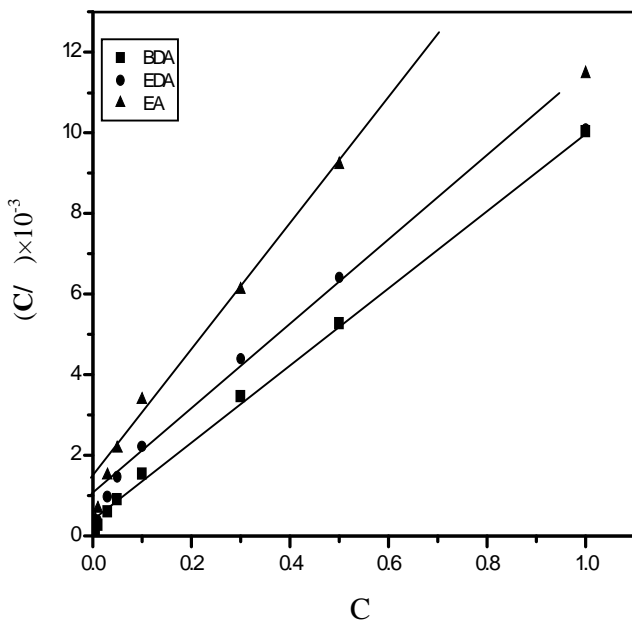


Fig. (9):Langmiur isotherm adsorption of BDA,EDA and EA on the surface of copper in 3M HNO₃ at 30°C.

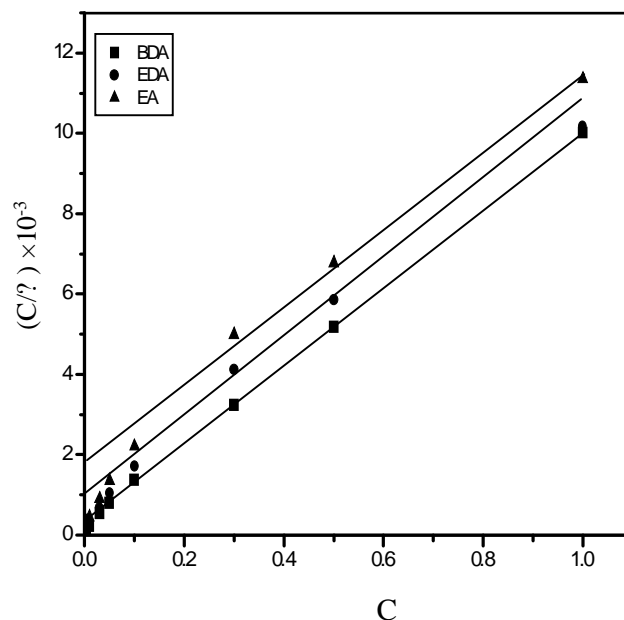


Fig.(10): Langmiur isotherm adsorption of BDA,EDA and EA on the surface of copper alloy in 3M HNO₃ at 30°C.

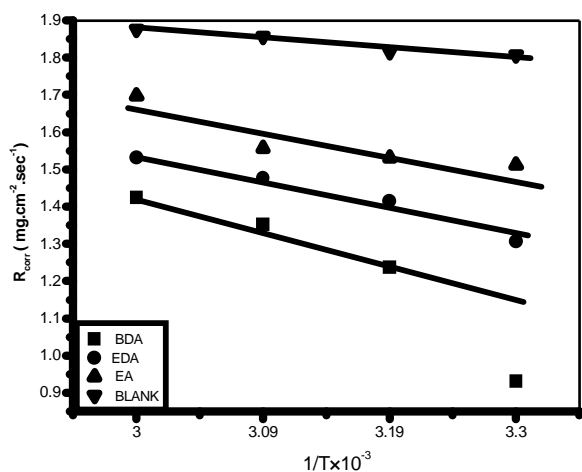


Fig.(11):Arrhenius plot of copper in 3M HNO₃ with and without BDA,EDA and EA.

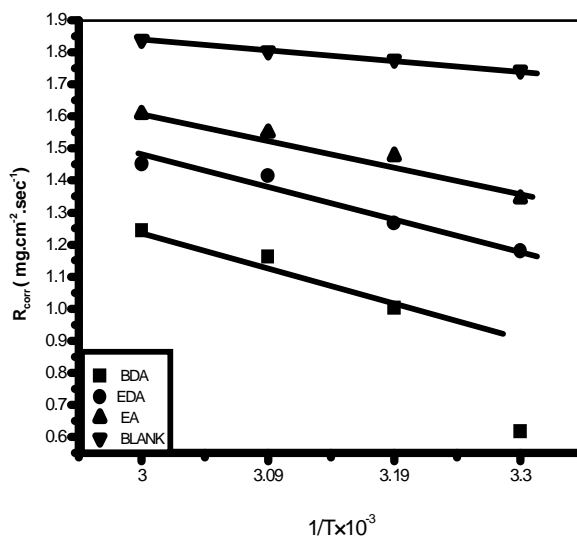


Fig.(12): Arrhenius plot of copper alloy in 3M HNO₃ with and without BDA,EDA and EA.

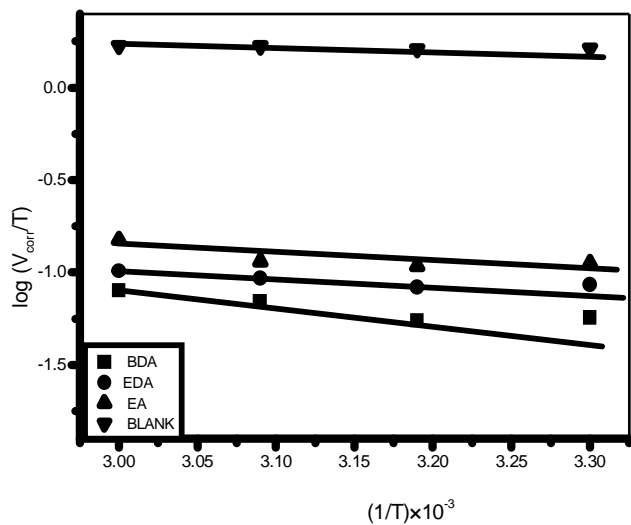


Fig.(13): log(V_{corr}/T) vs. (1/T)of copper in 3M HNO₃ in presence and absence of BDA, EDA and EA.

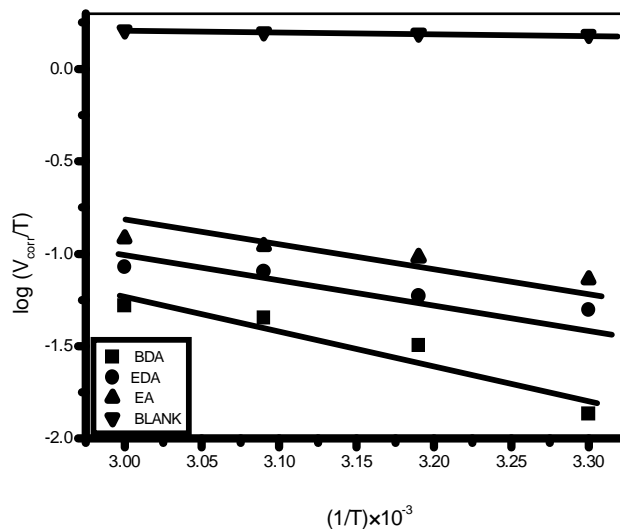


Fig.(14): log(V_{corr}/T) vs.(1/T)of copper alloy in 3M HNO₃ in presence and absence of BDA, EDA and EA.

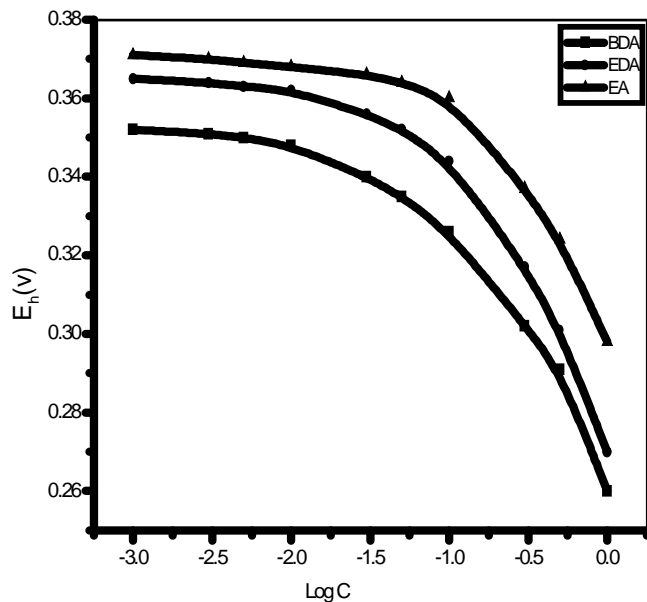


Fig.(15):the steady state potential of copper E_h vs. the logarithm of different concentrations of tested inhibitor in 3M HNO_3 .

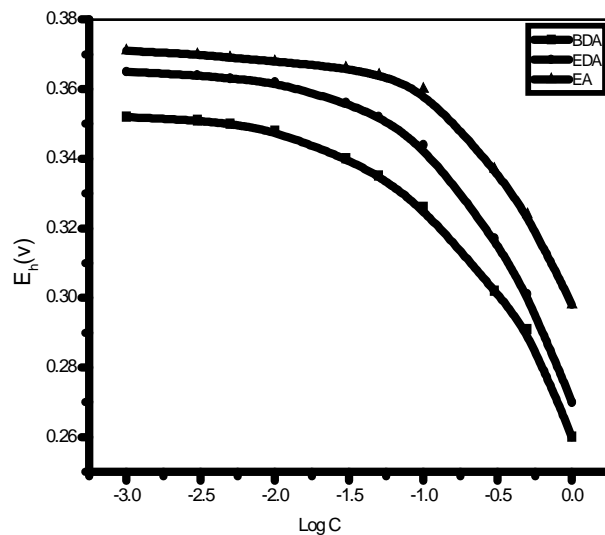


Fig.(16): the steady state potential of copper alloy (E_h) vs. the logarithm of different concentrations of tested inhibitor in 3M HNO_3 .

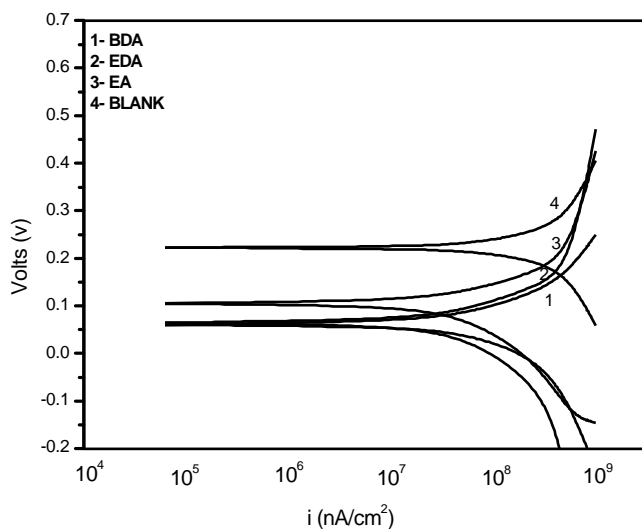


Fig.(17): Potentiodynamic polarization curves of copper in 3M HNO_3 in absence and presences of the tested inhibitors.

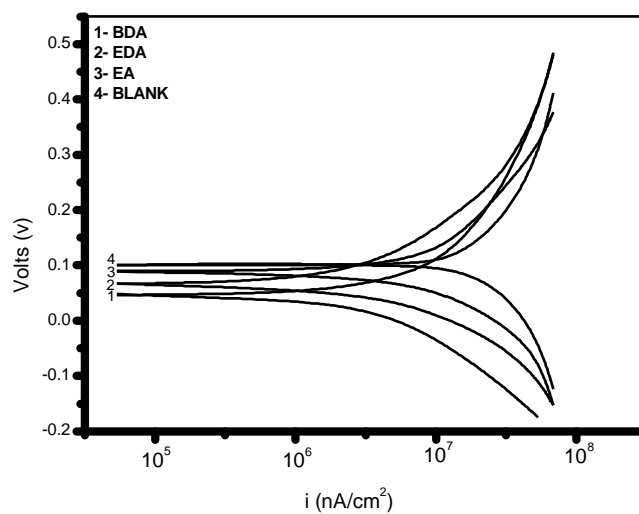


Fig.(18): Potentiodynamic polarization curves of copper alloy in 3M HNO_3 in absence and presences of the tested inhibitors.

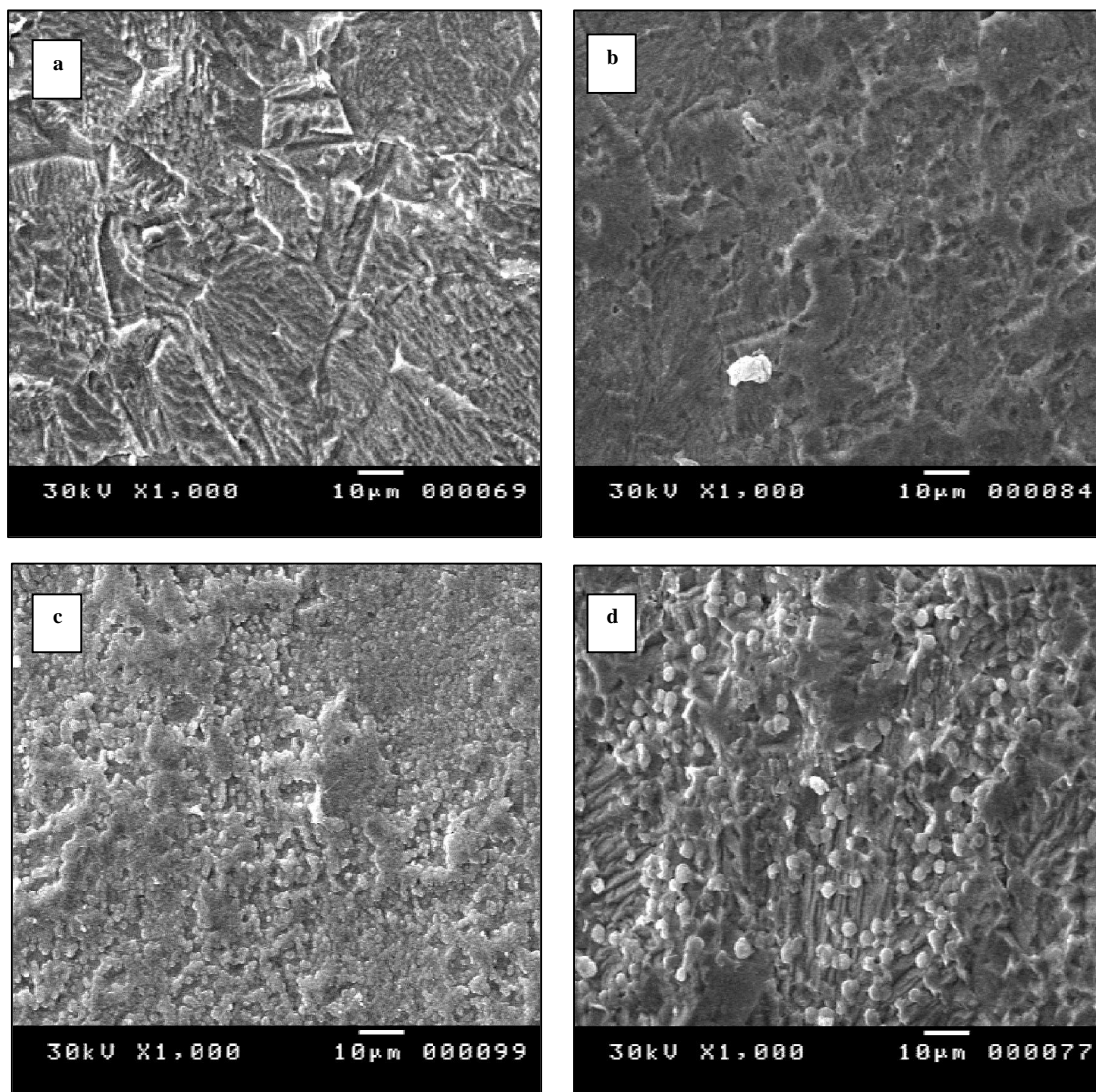


Fig.(19): Scanning electron microscope of copper in free acid (a) and in presence of BDA (b), EDA (c) and EA(d).

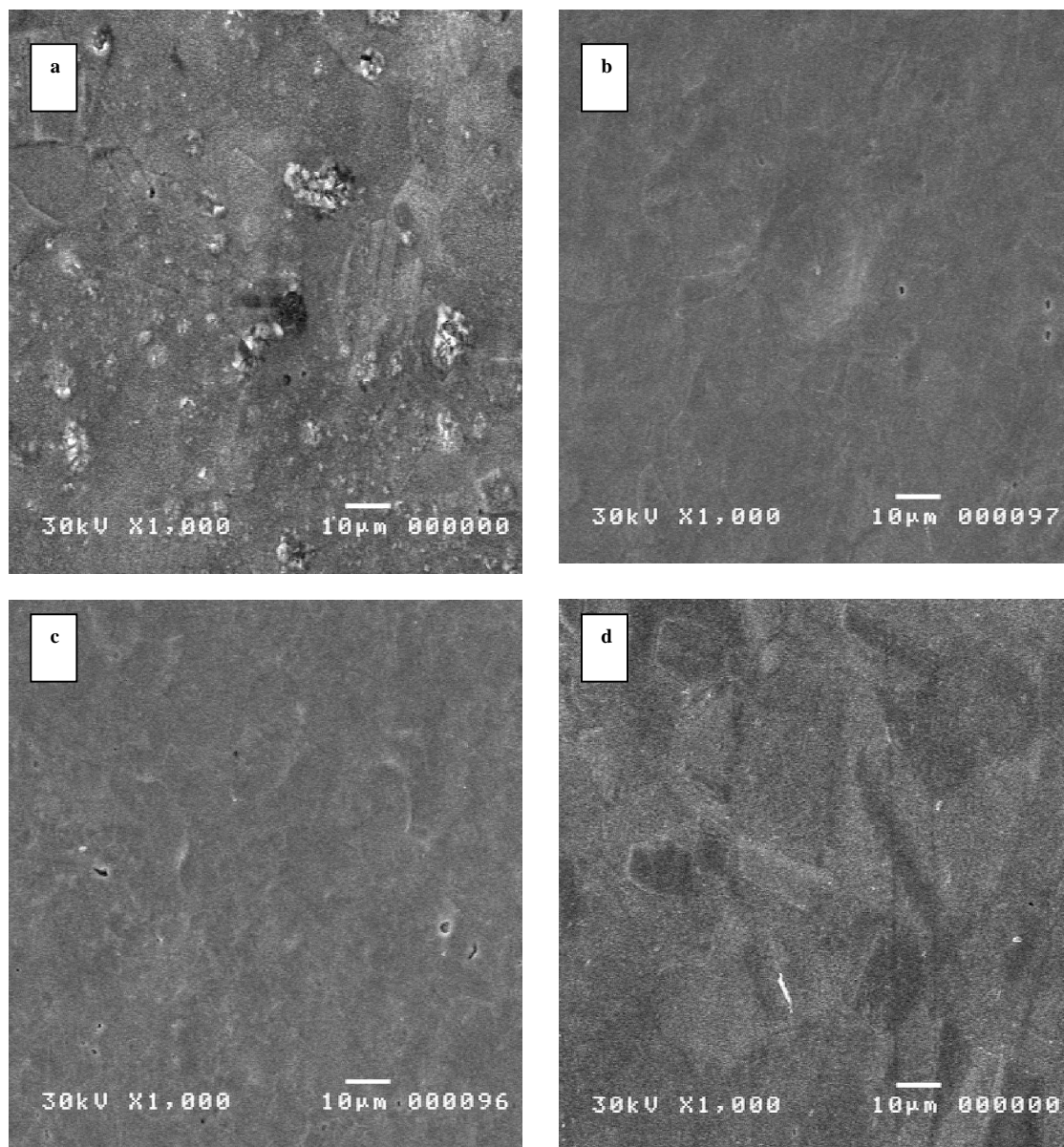


Fig.(20): Scanning electron microscope of copper alloy in free acid (a) and in presence of BDA (b), EDA (c) and EA(d).

4. Conclusion

The corrosion rate of copper is greater than copper alloy in the corrosive medium with or without the addition of the inhibitor.

The addition of BDA, EDA or EA has strong inhibiting effect for copper and copper alloy dissolution in 3M nitric acid solution, and the protection efficiency follows the order BDA > EDA > EA.

The protection efficiency of BDA and EDA are very similar, at higher inhibitor concentration, 99.6% and 99.07% respectively.

The adsorption of BDA, EDA and EA on copper and copper alloy followed a physical adsorption.

Corresponding author

O.R.M. Khalifa

Chemistry department, Faculty of Girls for Arts, Science and Education, Ain shams University, Cairo, Egypt

5. References

1. H. Leidheiser, (1979) "Aqueous Corrosion" in The Corrosion of Copper, Tin and Their Alloys, Robert E. Krieger Publishing Company, Huntington, NY, pp. 71 – 126.
2. U.R. Evans, Behaviour of metals in nitric acid, Trans. Farad. Soc. 40 (1944) 120.
3. C.N. Hinshelwood, Presidential address. Some observations on present day chemical kinetics, J. Chem. Soc. (1947) 694.
4. E.A. Travincek, J.H. Weber, Continuous dissolution of copper by nitric ACID, J. Phys. Chem. 65 (1961) 235.
5. Rasheed Arain, A.M. Shams El Din, A thermometric study of the kinetics of acid dissolution of four copper alloys used in desalination plants, Thermochim. Acta 89 (1985) 171.
6. M. Sato, R. Aogaki, Electrochemical Methods in Corrosion Research VI, Mater. Sci. Forum 289–292 (1998) 459.
7. D.-Q. Zhang, L.-X. Gao, G.-D. Zhou, Inhibition of copper corrosion by bis-(1-benzotriazolymethylene)-(2,5-thiadiazoly)-disulfide in chloride media, J. Appl. Surf. Sci. 225 (2004)287.
8. D.-Q. Zhang, L.-X. Gao, G.-D. Zhou, Inhibition of copper corrosion in aerated hydrochloric acid solution by heterocyclic compounds containing a mercapto group, Corros. Sci. 46 (2004) 3031.
9. D.-Q. Zhang, L.-X. Gao, G.-D. Zhou, Synergistic effect of 2-mercapto benzimidazole and KI on copper corrosion inhibition in aerated sulfuric acid solution, J. Appl. Electrochem. 33 (2003) 361.
10. A.G. Christy, A. Lowe, V. Otieno-Alego, M. Stoll, R.D. Webster, Voltammetric and Raman microspectroscopic studies on artificial copper pits grown in simulated potable water, J. Appl. Electrochem. 34 (2004) 225.
11. H. Otmacic, J. Telegdi, K. Papp, E. Stupnisek-Lisac, Protective Properties of An Inhibitor Layer Formed on Copper in Neutral Chloride Solution, J. Appl. Electrochem. 34 (2004) 545.
12. H. Ma, S. Chen, L. Niu, S. Zhao, S. Li, D. Li, Inhibition of copper corrosion by several Schiff bases in aerated halide solutions, J. Appl. Electrochem. 32 (2002) 65.
13. F. Zucchi, G. Trabaneli, M. Fonsati, Tetrazole derivatives as corrosion inhibitors for copper in chloride solutions, Corros. Sci. 38 (1996) 2019.
14. Wang, S. Chen, S. Zhao, Inhibition Effect of AC-Treated, Mixed Self-Assembled Film of Phenylthiourea and 1-Dodecanethiol on Copper Corrosion, J. Electrochem. Soc. 151 (2004) B11.
15. M. Kendig, S. Jeanjaquet, Cr(VI) and Ce(III) Inhibition of Oxygen Reduction on Copper, J. Electrochem. Soc. 149 (2002) B47.
16. H.Y. Ma, C. Yang, B.S. Yin, G.Y. Li, S.H. Chen, J.L. Luo, Electrochemical characterization of copper surface modified by n-alkanethiols in chloride-containing solutions, J. Appl. Surf. Sci. 218 (2003) 143.
17. G.K. Gomma, M.H. Wahdan, Effect of temperature on the acidic dissolution of copper in the presence of amino acids Mater. Chem. Phys. 39 (1994) 142.
18. K.F. Khaled, N. Hackerman, Ortho-substituted anilines to inhibit copper corrosion in aerated 0.5 M hydrochloric acid, Electrochem. Acta 49 (2004) 485.
19. H. Otmacic, E. Stupnisek-Lisac, Copper corrosion inhibitors in near neutral media, Electrochim. Acta 48 (2002) 985.
20. M.A. Elmorsi, A.M. Hassanein, Corrosion inhibition of copper by heterocyclic compounds Corros. Sci. 41 (1999) 2337.
21. M. Scendo, D. Poddebniak, J. Malyszko, Indole and 5-chloroindole as inhibitors of anodic dissolution and cathodic deposition of copper in acidic chloride solutions, J. Appl. Electrochem. 33(2003) 287.
22. Dafali, B. Hammouti, R. Touzani, S. Kertit, A. Ramdani, K. El Kacemi, corrosion inhibition of copper in 3 per cent NaCl solution by new bipyrazolic derivatives, Anti-Corros. Methods Mater. 49 (2002) 96.
23. F.M. Al-Kharafi, 2-amino-thiazole and 2-amino-4,6-dimethylpyrimidine as corrosion inhibitors for copper Corros. Sci. 28 (1988) 163.

24. M.G. Fontana, K.W. Staehle, *Advances in Corrosion Science and Technology*, vol. 1, Plenum Press, New York, 1970.
25. O.L. Riggs Jr., in: C.C. Nathan (Ed.), *Corrosion Inhibitors*, second ed., NACE (National Association of Corrosion Engineers), Houston, TX, 1973.
26. R.D. Srivastafa, R.C. Mukerjee, A.K. Agarwal, Corrosion of electroplated Cu---Cd alloys and its inhibition, *Corros. Sci.* 19 (1979) 27.
27. F.H.Asaf,M.Aboukrisha,M.khodari,F.Echeihk,A. A.Hussien, Studies on dissolution and inhibition of copper in nitric acid using stripping voltammetry and conductance measurement, *Mater.chem.Phys.*9313(2002).
28. E.A.Noor, The inhibition of mild steel corrosion in phosphoric acid solutions by some N-heterocyclic compounds in the salt form ,*corros.sci*47(2005)33.
29. M.K. Gomma and M. H Wadan, Schiff bases as corrosion inhibitors for aluminium in hydrochloric acid solution, *Materials Chemistry and physics*,39(1995)209.
30. J.Marsh, *Advanced organic Chemistry*, 3rd ed., Wiley Eastern, New Dielhi(1988).
31. E. E. Ebenso, Hailemichael Alemu 1, S. A. Umoren 2 and I.B. Obot 2 Int., Inhibition of Mild Steel Corrosion in Sulphuric Acid Using Alizarin Yellow GG Dye and Synergistic Iodide Additive *J. Electrochem. Sci.*, 3 (2008) 1325 – 133.

7/8/2010